Surface Interaction Forces of Well-Defined, High-Density Polymer Brushes Studied by Atomic Force Microscopy. 1. Effect of Chain Length

Shinpei Yamamoto, Muhammad Ejaz, Yoshinobu Tsujii, Mutsuo Matsumoto, and Takeshi Fukuda*

Institute for Chemical Research, Kyoto University, Uji, Kyoto 611-0011, Japan

Received October 18, 1999; Revised Manuscript Received April 24, 2000

ABSTRACT: We made direct force measurements by atomic force microscopy (AFM) at surfaces of polymer brushes comprised of low-polydispersity poly(methyl methacrylate) (PMMA) chains densely end-grafted on a silicon substrate by living radical polymerization. These brushes are characterized by an exceptionally high, nearly constant graft density (approximately 0.4 chains/nm^2) and a wide range of molecular weights of the graft chains. This graft density is at least 10 times larger than those of the previously studied polymer brushes prepared by the adsorption of block copolymers. Force measurements were made in toluene with a silica particle-attached cantilever. The hysteresis behavior of a piezo actuator used in the AFM was corrected by simultaneously measuring its piezo current. The true distance D between the substrate surface and the silica probe, which usually is difficult to define in AFM experiments, was successfully determined by AFM imaging across the boundary of a scratched and an unscratched region on the sample surface. In this way, we could obtain quantitative force−distance profiles. The repulsive force was observed to rapidly increase with decreasing separation. The equilibrium thickness L_e of the brushes, i.e., the critical distance at which a repulsive force was detectable, was found to be proportional to the weight-average chain contour length $L_{c,w}$, giving $L_e/L_{c,w} = 0.6$. This indicates formation of a homogeneous polymer layer with highly stretched graft chains. Unlike the previously reported results for lower density polymer brushes, the force−distance profiles for different graft chain lengths were not scaled by the reduced distance D/L_e. Longer brushes were more resistant to compression: for example, the longest studied brush was compressible only to $D/L_e = 0.8$, which was about 3 times as large as the scaled dry thickness L_d/L_e.

Introduction

Polymers end-grafted on a solid surface play an important role in many areas of science and technology, e.g., colloid stabilization, adhesion, lubrication, tribology, and rheology.[1−5] The conformation of those polymers in a good solvent can dramatically change with graft density;[6−8] at low graft densities, a "mushroom" structure will be formed with the coil dimension similar to that of ungrafted chains. With increasing graft density, graft chains will be obliged to stretch away from the surface, forming a so-called "polymer brush". Polymer brushes have been extensively studied: for example, the brush height and the segment density profile in a good solvent were studied by neutron reflectometry,[9−11] and the forces at polymer brush surfaces were directly measured by a surface force apparatus (SFA)[12−14] and an atomic force microscope (AFM).[15−18]

Most of the polymer brushes experimentally studied so far were prepared by end-functionalized polymers or block copolymers with terminal group or one block selectively adsorbed on the surface. These systems, however, had a rather low graft density, typically 0.001−0.05 chains/nm^2. These graft densities correspond to the "moderate density" regime, in which graft chains overlap each other, but the volume fraction of polymer in the layer is still so low that the interaction free energy is dominated by binary interactions and the elastic free energy is approximately Gaussian. Theoretical analyses of polymer brushes with higher graft densities which take account of higher-order interactions predict that the repulsive force steeply increases with increasing graft density.[19,20] By the adsorption procedure with preformed polymers, however, it is difficult to obtain such high graft densities.[21] An alternative method is the graft polymerization starting with initiating sites fixed on a surface, but it usually results in a poor control of chain length and its distribution.[23−25] Recently, living polymerization techniques were successfully applied to the surface-initiated graft polymerization to prepare a dense polymer brush with these parameters controlled.[26−31] Some research groups[27−31] have explored the applicability of living radical polymerization (LRP), which has been attracting much attention as a new route to well-defined polymers with low polydispersities.[32] Its clear advantage over other polymerization techniques may be the applicability to a large variety of monomers without involved procedures including perfect removal of water and other impurities and protection and deprotection of reactive groups. We were the first to succeed in preparing a low-polydispersity polymer brush with an exceptionally high graft density on a silicon substrate,[27] in which we made a combined use of two independent techniques: one was the Langmuir−Blodgett (LB) technique[33] to provide a well-organized set of initiating sites on the surface, and the other was the atom transfer radical polymerization (ATRP) technique,[34] a variant of LRP, to achieve a controlled graft polymerization.

In this work, we have made an AFM study on the structure and interaction forces of poly(methyl methacrylate) (PMMA) brushes prepared by the surface-initiated ATRP technique. The graft density of the studied PMMA brushes was estimated to be as high as 0.4 chains/nm^2, which is one of the highest ever reported

* To whom correspondence should be addressed: e-mail fukuda@scl.kyoto-u.ac.jp.

10.1021/ma991733a CCC: $19.00
Published on Web 07/06/2000

Table 1. Characteristics of the PMMA Brushes

sample	L_d (nm)[a]	M_n[b]	M_w/M_n[b]
C1	12	23 000	1.36
C2	20	35 900	1.36
C3	44	70 500	1.34
C4	87	121 700	1.39
C5	102	171 400	1.56

[a] Thickness in dry state. [b] Values for the free polymers produced in solution (see text).

values, being an order of magnitude larger than those of the polymer brushes prepared by the adsorption method. While the AFM method is advantageous over the SFA technique in some respects, it has two problems to be solved for the use of quantitative analysis. One is the hysteresis behavior of the piezo actuator controlled by an applied voltage. The other is the general difficulty of determining the exact distance (separation) between surfaces, since an AFM tip cannot reach a densely covered substrate surface. We have succeeded in solving these problems, as will be described below.

Experimental Section

Preparation and Characterization of Polymer Brushes. The PMMA brushes were prepared by the surface-initiated ATRP technique according to the procedures described elsewhere.[27] In brief, the initiator, 2-(4-chlorosulfonylphenyl)-ethyltrimethoxysilane (Gelest, Inc., USA), was deposited on a cleaned silicon wafer by the LB technique and immobilized by thermal treatment. The graft polymerization was carried out at 90 °C for various periods of time in a degassed diphenyl ether solution containing CuBr (10 mM), 4,4′-di-*n*-heptyl-2,2′-bipyridine (20 mM), methyl methacrylate (4.7 M), and *p*-toluenesulfonyl chloride (TsCl, 3.6 mM). TsCl was added as a free initiator not only to control the polymerization but also to produce free polymers, which are useful as a measure of the molecular weight and molecular weight distribution of the graft chains.[27] After polymerization, the substrate was rinsed in a Soxhlet extractor with toluene for 12 h to remove physisorbed polymers and impurities. The AFM observation in the air revealed the formation of a homogeneous graft (brush) layer on the substrate. The layer thickness L_d in a dry state was determined by ellipsometry (a DVA ellipsometer, Mizojiri Optical Co., Ltd., Japan). Table 1 summarizes the characteristics of the PMMA brushes prepared in this study. In the table, the number-average molecular weight (M_n) and the polydispersity index (M_w/M_n) are those of the free polymers produced in the solution, determined by the PMMA-calibrated gel permeation chromatographic analysis. There are reasons to believe that these values should well approximate those of the graft chains.[27,35]

Figure 1 shows that the dry thickness L_d is proportional to M_n, suggesting that the graft density is effectively constant independent of chain length. The slope of the line shows that the graft density is as high as about 0.4 chains/nm^2.[36]

AFM Measurements. Topographic imaging and force measurements were performed by an atomic force microscope (Seiko Instruments Inc., Japan, SPI3600) with a V-shaped cantilever (Olympus Optical CO., Ltd., Japan, spring constant 0.16 N/m). The spring constants of several cantilevers were measured according to the method of Cleaveland et al.,[38] and the obtained values were found to be within ±10% of the company-given value. This much of an error in the spring constant has no serious effect on the experimental data: for example, this causes an error less than 1% in the equilibrium thickness L_e. A liquid cell was used for the measurement in toluene, which is a good solvent for PMMA. Toluene (Spectrograde, Dojindo Laboratories, Japan) was used without further purification.

Interaction forces between the PMMA brush and the silica sphere attached to the cantilever as a probe were measured in toluene as a function of separation using a modified SPI3600 AFM apparatus. To move the sample stage, a piezo actuator of one-dimensional layered type (Taiheiyo Cement, CO., Japan, PMF-2020 controlled by the piezo driver PM-1100) was installed in the AFM instead of the three-dimensional piezo actuator used for imaging. The one-dimensional piezo actuator gives less angular (bending) motion that causes deviations from the *z* axis. The hysteresis effect of the piezo actuator was corrected as will be described below. The silica sphere (Ube Nitto Kasei, Japan, diameter 5 μm) was glued as a probe to the cantilever with a small amount of resin (Ciba-Geigy, Swiss, Araldite), which was confirmed to be inert under the measurement condition.[39,40] Immediately prior to each force measurement, the silica probe fixed on the cantilever was immersed in a solution of dimethyldichlorosilane/toluene (1:3 by weight) for 30 min to make the surface hydrophobic. A hydrophobically treated Si substrate was also prepared by the same way. The brush samples were cleaned by rinsing with copious amounts of the solvent and mounted on the piezo actuator. The solvent was injected into the liquid cell, and the brushes were allowed to be equilibrated in the solvent for 20 min. Then, the deflection of the cantilever with a silica probe was determined by the laser beam deflection technique and recorded as a function of the displacement of the piezo actuator while the sample was continuously moved up and down. These cantilever deflection vs displacement data were converted into the reduced force (F/R, see below) vs separation data following the principle of Ducker et al.,[39] which requires zeros of both force and separation to be defined. The zero of force was chosen at separations where the sample and the silica probe were far enough apart, and the zero of separation was chosen in the so-called constant-compliance region where the cantilever deflection increased linearly with decreasing separations. Typically, force curves were collected with a scan rate of 0.5 Hz, and a total of 30 force curves were taken at different locations on each sample.

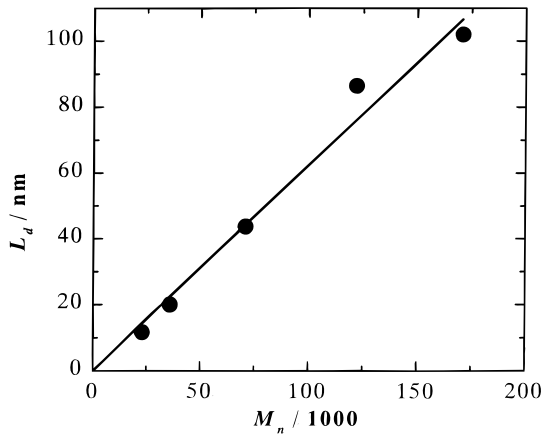

Figure 1. Relationship between dry thickness L_d of polymer brushes and M_n of free polymers produced in solution.

Calibration of Piezo Actuator. The displacements of piezo actuators used in AFM are usually controlled by the voltage applied to the actuators. In this case, however, the problem is the hysteresis effect that the displacement does not change linearly with the applied voltage.[41] This is a serious problem for the force measurement but not for imaging, since the former requires a relatively large change in displacement. Comstock[42] reported that, by controlling the charge applied on the actuator, the hysteresis can be reduced and a more linear input−displacement response can be achieved. This means that the hysteresis in the voltage−displacement response can be corrected by the charge applied on the actuator.

The piezo actuator of one-dimensional layered type used in the force measurement was calibrated as follows: when the voltage with a triangular waveform was applied on the actuator, the displacement was measured by the interferometric method,[43] in which we used a half mirror instead of a cantilever to measure the interference between the fixed half mirror and the mirror mounted on the piezo actuator. Simul-

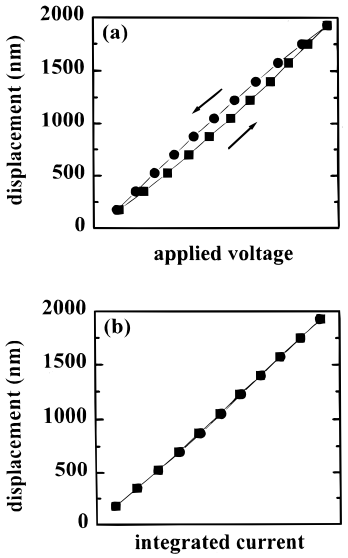

Figure 2. Displacement change plotted as a function of (a) the applied voltage and (b) the integrated current.

taneously, we measured the piezo current passing through the driving circuit of the actuator. The integrated current should correspond to the change in charge on the actuator, because the actuator has a resistance larger than 100 MΩ, and hence the leak current in the actuator can be ignored under the measurement condition. Parts a and b of Figure 2 show the displacement as a function of the applied voltage and the integrated current, respectively. Although the voltage vs displacement curve gives a hysteresis, the displacement changes approximately linearly with the integrated current. The slope of the line, which corresponds to the conversion factor between the integrated current and the displacement, was almost independent of the scan range and frequency studied here. Therefore, the piezo current was simultaneously measured in the force measurement, and the displacement of the piezo actuator was corrected by the integrated current with this conversion factor.

Results and Discussion

Force−Distance Profiles. The interaction forces of solvent-swollen PMMA brushes compressed by the probe sphere were measured in toluene. The measured force F can be reduced to the free energy G_f of interactions between two parallel plates according to the Derjaguin approximation, $F/R = 2\pi G_f$, where R is the radius of the probe sphere. Figure 3 shows the F/R vs separation D' profiles (force curves) measured in the advancing mode (the probe sphere approaching the brush). The F/R value increased with decreasing D'. Essentially no interaction force was observed for the bare silicon substrate with a hydrophobic surface. Thus, the observed repulsive forces originate from the steric interaction between the solvent-swollen PMMA brush and the probe sphere.

It should be noted that the separation D' estimated by the AFM force measurement is not the distance from the substrate surface but that from the constant compliance region where the cantilever deflection was proportional to the piezo displacement. In other words, the zero of D' was defined as the critical plane beyond which the sample was no more compressible. In a system with a dense polymer layer, for example, the distance between the $D' = 0$ plane and the substrate surface, which is called the "offset distance", can be very large, but there has been proposed no useful method to determine this

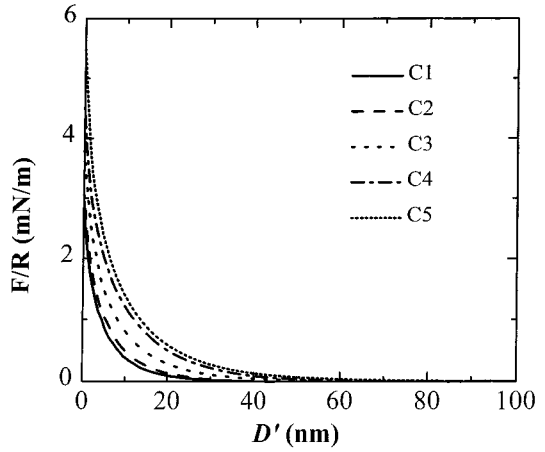

Figure 3. F/R vs D' curves of the PMMA brushes. The zero of D' is defined at the constant compliance region. These force profiles are the averaged ones.

Table 2. Offset (Uncompressible) Distance D_o and Equilibrium Thickness L_e of PMMA Brushes

sample	D_o (nm)	L_e (nm)	sample	D_o (nm)	L_e (nm)
C1	12 ± 0.3	53	C4	215 ± 20	295
C2	56 ± 7	109	C5	293 ± 10	386
C3	110 ± 15	185			

distance. (Recently, Butt et al., who measured a similar long-ranged repulsive force between an AFM tip and a polystyrene brush prepared by the conventional free radical polymerization, attempted to determine the offset distance by analyzing the force profile, with very limited success.[44])

Here we measured the offset distance D_o as follows: by using tweezers, we gave a scratch on the substrate surface to remove the polymer layer on it and observed it by AFM with the probe sphere-attached cantilever scanned across the scratch boundary. In this way, we could measure the difference in height between the unscratched and scratched regions. In the dry state, this difference agreed with the dry thickness L_d determined by ellipsometry. This means that in the scratched area the PMMA brushes were completely removed without damaging the substrate surface. To evaluate the offset distance D_o, AFM images were similarly taken in toluene under a constant force mode by applying the force corresponding to the constant compliance region in the force measurement.[45] Such an image is shown in Figure 4. Images at more than 20 different locations were taken for each sample.

Table 2 displays the average values of D_o along with the standard deviations for all the studied polymer brushes. The true distance D between the surfaces of the substrate and the probe sphere may be given by

$$D = D' + D_o \tag{1}$$

Figure 5 shows the corrected force curves, i.e., the F/R vs D curves, which are surprisingly different from the F/R vs D' curves in Figure 3. The most notable feature of the F/R vs D curves is a rapid increase of the repulsive force with decreasing D; that is to say, these PMMA brushes are highly resistant to compression.

Equilibrium Thickness of Polymer Brush. The successful determination of D_o and hence D enables us to estimate the equilibrium thickness L_e of the solvent-swollen brushes, where L_e is the critical distance at which a repulsive force is detectable (cf. Figure 5). In

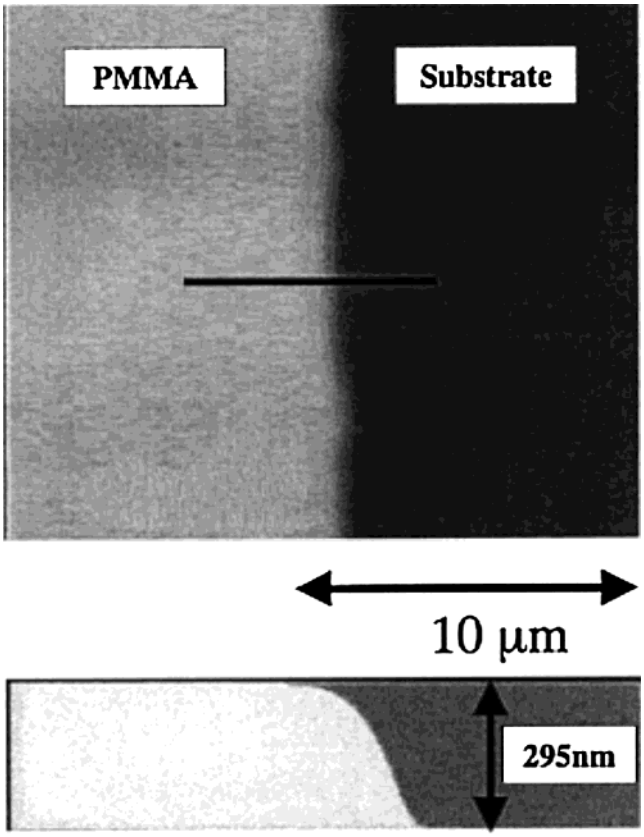

Figure 4. Typical topographic and cross-sectional AFM image across the boundary between the scratched and unscratched parts of the PMMA brush (C5). The image was taken under constant force mode by using the probe-attached cantilever in toluene.

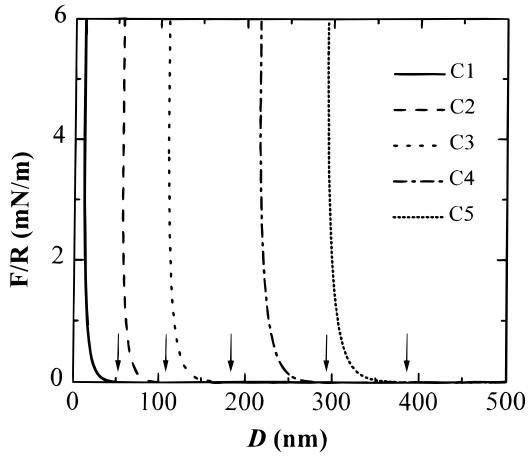

Figure 5. *F*/*R* vs *D* curves of the PMMA brushes. The zero of *D* is the substrate surface. The arrowheads indicate L_e.

the high surface density regime $s \ll R_F$, where s is the average distance between graft points (more specifically, we define s^2 as the surface area occupied by a graft chain) and R_F is the Flory radius of a free chain with the same degree of polymerization, N, as the graft chain, the graft chains in a good solvent will get extended away from the surface to decrease the interaction energy between polymer segments. On the other hand, the elastic free energy of the chain will increase by stretching. By minimizing the overall free energy with respect to the thickness of polymer layer, the scaling[46] and self-consistent mean-field approaches[47] predict that L_e varies like

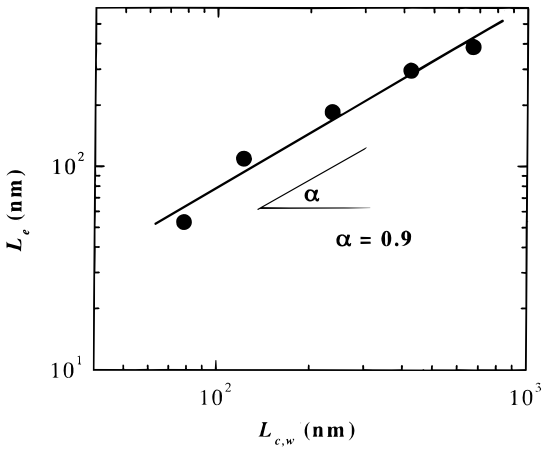

Figure 6. Plot of the equilibrium thickness L_e vs the contour length $L_{c,w}$.

$$L_e \propto Ns^{-2/3}a^{5/3} = Na\sigma^{*1/3} = L_c\sigma^{*1/3} \quad (\sigma^* = a^2/s^2) \quad (2)$$

where σ^* is the dimensionless surface density given by the number of graft chains per monomer cross section a^2, and L_c is the contour length of the graft chain. This relationship was confirmed by other theoretical calculations as well as by some experimental data for polymer brushes. Since the graft density is almost constant independent of chain length in our system (see above), a linear dependence of L_e on N is expected from the theory. In Figure 6, L_e is plotted against $L_{c,w}$ on logarithmic scale, where $L_{c,w}$ is the weight-average contour length calculated from the M_w value and the contour length of monomer unit (0.25 nm). The weight average, rather than the number average, was adopted by referring to the studies of Milner et al.,[47] in which a (moderate-density) polymer brush with a *uniform* distribution in chain length ($M_w/M_n > 1$) was predicted to be thicker than the equivalent monodisperse brush with the same M_n by a factor of $1 + \{^3/_4(M_w/M_n - 1)\}^{1/2}$. According to this relation, our brushes can be approximated with an error of about 10% in L_e by monodisperse brushes with a chain length M_w. Figure 6 gives a linear line with a slope of 0.9. This confirms the proportionality of L_e to L_c (eq 2).

It should be noted that the ratio of L_e to $L_{c,w}$ in our system gives a nearly constant value, $L_e/L_{c,w} \approx 0.6$, independent of $L_{c,w}$. This value is very high compared with, e.g., $L_e/L_{c,w} = 0.3$, the value previously reported for the polymer brushes prepared by the adsorption of block copolymers.[48] This difference can be attributed to the difference in graft density: eq 2 with a missing prefactor of order unity approximately predicts that $L_e/L_c \approx \sigma^{*1/3}$, which gives $L_e/L_c = 0.7$ for our system with a graft density of about 0.4 chains/nm^2 (corresponding to $\sigma^* = {}^1/_3$; see above) and $L_e/L_c = 0.3$ for the block copolymer brushes with a graft density 10 times lower than that of our system.

Compressibility of Polymer Brush. Using the scaling approach, de Gennes[49] derived the following equation concerning the interaction force f between two parallel plates with a relatively dense polymer brush layer:

$$f(D) \propto s^{-3}[(L_e/D)^{9/4} - (D/L_e)^{3/4}] \quad (3)$$

where $2L_e$ in the original formulation was replaced by L_e because only one surface was covered by the brush

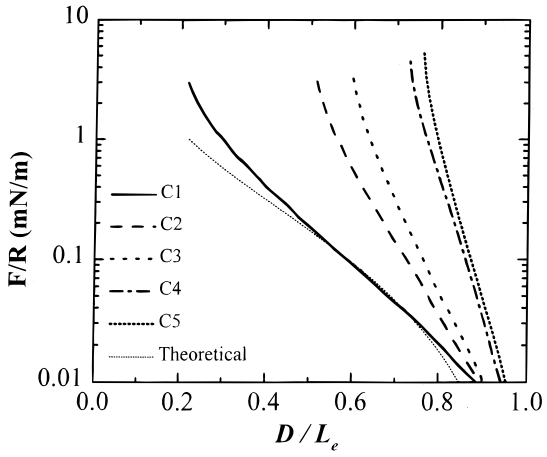

Figure 7. Scaled force profiles (F/R vs D/L_e curves) plotted in semilogarithmic scale.

layer in our case. This equation is integrated from L_e to D, giving the interaction free energy G_f between two parallel plates, which is related to the measured F/R values according to the Derjaguin approximation:

$$F/R = 2\pi G_f = 2\pi \int_{L_e}^{D} f(D)\, dD \qquad (4)$$

Equations 3 and 4 predict that the F/R value should be scaled by D/L_e for the polymer brushes with the same graft density (constant s). The force−distance profiles previously reported for the block copolymer brushes were nearly consistent with this scaling theory.

Figure 7 shows the F/R vs D/L_e plot for our system. Clearly, our system is poorly represented by the scaling theory. This indicates that the graft density in our system is so high that eq 3 is no longer applicable: this equation was derived for polymer brushes with a "moderately high" graft density, in which graft chains overlap each other but the volume fraction of polymer in the layer is still low enough so that the "binary interaction" and the "Gaussian elastic free energy" approximations are valid. Figure 7 reveals that the scaled force−distance profile strongly depends on the chain length. In the case of the shortest graft chain (C1), the brush layer was compressible nearly to the dry thickness (the dry thickness L_d scaled by L_e, i.e., the ratio L_d/L_e was nearly constant in all cases). With increasing chain length, the scaled force curve becomes steeper, meaning that the brush layer becomes more and more difficult to be compressed. The system with the longest graft chain (C5) was compressible only to D/L_e ($=D_o/L_e$) = 0.8, which is about 3 times larger than the dry thickness, $L_d/L_e = 0.26$ (cf. Table 1). This strong resistance against compression must be characteristic of polymer brushes with an extremely high graft density. In the case of such a dense polymer brush with long graft chains, the relaxation processes of graft chains might affect the force−distance profile. These dynamic properties of dense polymer brushes will be the topic of a forthcoming paper.

Conclusions

By the AFM force measurement using a silica probe, we studied the structure and interaction forces, in toluene, of low-polydispersity PMMA brushes with an exceptionally high graft density (approximately 0.4 chains/nm^2), which is at least an order of magnitude larger than those of the previously studied polymer brushes prepared by the adsorption of block copolymers. Here, we succeeded in solving the two problems intrinsic to the AFM force measurement; the hysteresis behavior of a piezo actuator used in the AFM was corrected by simultaneously measuring its piezo current, and the true distance between the substrate surface and the silica probe was successfully determined by AFM imaging across the boundary of a scratched and an unscratched region of the sample surface. The obtained reduced force (F/R)−distance (D) profiles disclosed the following features: (i) the equilibrium thickness L_e of the brushes is proportional to the chain contour length $L_{c,w}$, giving $L_e/L_{c,w} = 0.6$ independent of $L_{c,w}$. This indicates that in our system the graft chains are highly stretched in toluene as compared with those prepared by the adsorption method, in which the graft densities are much lower, e.g., $L_e/L_{c,w} = 0.3$. (ii) The repulsive force rapidly increases with decreasing separation, and the F/R vs D profiles are not scaled by D/L_e, as have been reported for lower-density polymer brushes, but dependent on the chain length. The brush with longer graft chains are more resistant to compression; for example, the longest brush (C5) is compressible only to $D/L_e = 0.8$, which is about 3 times larger than the dry thickness. The strong resistance against compression must be characteristic of polymer brushes with an extremely high graft density.

Acknowledgment. The Research Fellowship of the Japan Society for the Promotion of Science for Young Scientists is gratefully acknowledged for partial financial support.

References and Notes

(1) Napper, D. H. *Polymeric Stabilization of Colloidal Dispersions*; Academic Press: London, 1983.
(2) Raphaël, E.; de Gennes, P. G. *J. Phys. Chem.* **1992**, *96*, 4002.
(3) Klein, J. *Annu. Rev. Mater. Sci.* **1996**, *26*, 581.
(4) Klein, J.; Kumacheva, E. *Science* **1995**, *269*, 816.
(5) Parnas, R. S.; Cohen, Y. *Rheol. Acta* **1994**, *33*, 485.
(6) Israelachvili, J. N. *Intermolecular and Surface Forces*, 2nd ed.; Academic Press: London, 1992.
(7) Halperin, A.; Tirrell, M.; Lodge, T. P. *Adv. Polym. Sci.* **1992**, *100*, 31.
(8) Kawaguchi, M.; Takahashi, A. *Adv. Colloid Interface Sci.* **1992**, *37*, 219.
(9) (a) Satija, S. K.; Majkrzak, C. F.; Russell, T. P.; Sinha, S. K.; Sirota, E. B.; Hughes, G. J. *Macromolecules* **1990**, *23*, 3860. (b) Levicky, R.; Koneripalli, N.: Tirrell, M.; Satija, S. K. *Macromolecules* **1998**, *31*, 3731.
(10) Cosgrove, T.; Heath, T. G.; Phipps, J. S.; Richardson, R. M. *Macromolecules* **1991**, *24*, 94.
(11) (a) Field, J. B.; Toprakcioglu, C.; Ball, R. C.; Stanley, H. B.; Dai, L.; Barfford, W.; Penfold, J.; Smith, G.; Hamilton, W. *Macromolecules* **1992**, *25*, 434. (b) Anastassopoulos, D. L.; Vradis, A. A.; Toprakcioglu, C.; Smith, G. S.; Dai, L. *Macromolecules* **1998**, *31*, 9369.
(12) (a) Hadziioannou, G.; Granick, S.; Patel, S.; Tirrell, M. *J. Am. Chem. Soc.* **1986**, *108*, 2869. (b) Watanabe, H.; Tirrell, M. *Macromolecules* **1993**, *26*, 6455.
(13) Ansarifer, A.; Luckham, P. F. *Polymer* **1988**, *29*, 329.
(14) Taunton, H. J.; Toprakcioglu, C.; Fetters, L.; Klein, J. *Macromolecules* **1990**, *23*, 571.
(15) Courvoisier, A.; Isel, F.; François, J.; Maaloum, M. *Langmuir* **1998**, *14*, 3727.
(16) Overney, R.; Leta, D.; Pictroski, C.; Rafailovich, M.; Liu, Y.; Quinn, J.; Sokolov, J.; Eisenberg, A.; Overney, G. *Phys. Rev. Lett.* **1996**, *76*, 1272.
(17) Kelley, T. W.; Schorr, P. A.; Johnson, K. D.; Tirrell, M.; Frisbie, C. D. *Macromolecules* **1998**, *31*, 4297.
(18) O'Shea, S. J.; Welland, M. E.; Rayment, T. *Langumir* **1993**, *9*, 1826.
(19) Shim, D. F. K.; Cates, M. E. *J. Phys. (Paris)* **1989**, *50*, 3535.

(20) Lai, P.-Y.; Halperin, A. *Macromolecules* **1991**, *24*, 4981.
(21) Higher graft densities were reported by Overney et al.[16] (ca. 0.1 chains/nm^2) and by Mansky et al.[22] (ca. 0.3 chains/nm^2). However, these values are considered to be attained because of very low molecular weight of adsorbed chains.
(22) Mansky, P.; Liu, Y.; Huang, E.; Russel, T. P.; Hawker, C. J. *Science* **1997**, *272*, 1458.
(23) Boven, G.; Oosterling, M. L. C. M.; Challa, G.; Jan, A. *Polymer* **1990**, *31*, 2377.
(24) (a) Tsubokawa, N.; Maruyama, K.; Sone, Y.; Shimomura, M. *Polym. J.* **1989**, *21*, 475. (b) Tsubokawa, N.; Shirai, Y.; Hashimoto, K. *Colloid Polym. Sci.* **1995**, *273*, 1049. (c) Tsubokawa, N.; Koshida, M. *J. Macromol. Sci., Pure Appl. Chem.* **1997**, *A34* (12), 2509.
(25) (a) Prucker, O.; Rühe, J. *Macromolecules* **1998**, *31*, 592. (b) Prucker, O.; Rühe, J. *Macromolecules* **1998**, *31*, 602.
(26) (a) Jordan, R.; Ulman, A. *J. Am. Chem. Soc.* **1998**, *120*, 243. (b) Jordan, R.; Ulman, A.; Kang, J. F.; Rafailovich, M. H.; Sokolov, J. *J. Am. Chem. Soc.* **1999**, *121*, 1016.
(27) Ejaz, M.; Yamamoto, S.; Ohno, K.; Tsujii, Y.; Fukuda, T. *Macromolecules* **1998**, *31*, 5934.
(28) Huang, X.; Wirth, M. J. *Macromolecules* **1999**, *32*, 1694.
(29) Zhao, B.; Brittain, W. J. *J. Am. Chem. Soc.* **1999**, *121*, 3557.
(30) Husseman, M.; Malmström, E. E.; McNamara, M.; Mate, M.; Mecerreyes, D.; Benoit, D. G.; Hedrick, J. L.; Mansky, P.; Huang, E.; Russell, T. P.; Hawker, C. J. *Macromolecules* **1999**, *32*, 1424.
(31) Matyjaszewski, K.; Miller, P. J.; Shukla, N.; Immaraporn, B.; Gelman, A,; Luokala, B. B.; Siclovan, T. M.; Kickelbick, G.; Vallant, T.; Hoffmann, H.; Pakula, T. *Macromolecules* **1999**, *32*, 8716.
(32) (a) Moad, G.; Rizzardo, E.; Solomon, D. H. In *Comprehensive Polymer Science*; Eastmond, G. C., Ledwith, A., Russo, S., Sigwalt, P., Eds.; Pergamon: Londo, 1989; Vol. 3, p 141. (b) Georges, M. K.; Veregin, R. P. N.; Kazmaier, P. M.; Hamer, G. K. *Trends Polym. Sci.* **1994**, *2*, 66. (c) Matyjaszewski, K.; Gaynor, S.; Greszta, D.; Mardare, D.; Shigemoto, T. *J. Phys. Org. Chem.* **1995**, *8*, 306. (d) Moad, G.; Solomon, D. H. *The Chemistry of Free Radical Polymerization*; Pergamon: Oxford, UK, 1995; p 335. (e) Davis, T. P.; Haddleton, D. M. In *New Methods of Polymer Synthesis*; Ebdon, J. R., Eastmond, G. C., Eds.; Blackie: Glasgow, UK, 1995; Vol. 2, p 1. (f) Hawker, C. J. *Trends Polym. Sci.* **1996**, *4*, 183. (g) Colombani, D. *Prog. Polym. Sci.* **1997**, *22*, 1649. (h) *Controlled Radical Polymerization*; Matyjaszewski, K., Ed.; ACS Symposium Series 685; American Chemical Society: Washington, DC, 1998. (i) Sawamoto, M.; Kamigaito, M. In *Polymer Synthesis*; Materials Science and Technology Series; VCH−Wiley: Weinheim, 1998; Chapter 1. (j) Otsu, T.; Mastumoto, A. *Adv. Polym. Sci.* **1998**, *136*, 75. (k) Fukuda, T.; Goto, A.; Ohno, K. *Macromol. Rapid Commun.* **2000**, *21*, 151.
(33) Ulman, A. *An Introduction to Ultrathin Organic Films from Langmuir−Blodgett to Self-Assembly*; Academic Press: San Diego, CA, 1991.
(34) (a) Wang, J. S.; Matyjaszewski, K. *J. Am. Chem. Soc.* **1995**, *117*, 5614. (b) Kato, M.; Kamigaito, M.; Sawamoto, T.; Higashimura, T. *Macromolecules* **1995**, *28*, 1721. (c) Percec, V.; Barboiu, B. *Macromolecules* **1995**, *28*, 7970. (d) Granel, C.; Dubois, Ph.; Jérôme, R.; Teyssié, Ph. *Macromolecules* **1996**, *29*, 8576. (e) Haddleton, D. M.; Jasieczek, C. B.; Hannon, M. J.; Scooter, A. J. *Macromolecules* **1997**, *30*, 2190. (f) Leduc, M. R.; Hayes, W.; Fréchet, J. M. J. *J. Polym. Sci., Part A: Polym. Chem.* **1998**, *36*, 1. (g) Jankova, K.; Chen, X.; Kops, J.; Batsberg, W. *Macromolecules* **1998**, *31*, 538. (h) Angot, S.; Murthy, K. S.; Taton, D.; Gnanou, Y. *Macromolecules* **1998**, *31*, 7218. (i) Ohno, K.; Goto, A.; Fukuda, T.; Xia, J.; Matyjaszewski, K. *Macromolecules* **1998**, *31*, 2699.
(35) To directly confirm this, the graft polymerization was carried out on initiator-fixed silica particles with larger surface area instead of a flat substrate, and the graft chains were cleaved by the treatment with a HF solution. GPC analysis confirmed that they have nearly the same molecular weight as the free polymer (unpublished data).
(36) The graft density of about 0.4 chains/nm^2 is smaller than the surface density of the initiator (about 4 molecules/nm^2) estimated from the surface pressure−occupied area isotherm.[27] This difference is to be ascribed to a steric effect in the surface-graft polymerization, which is discussed in more details in a forthcoming paper.[37]
(37) Yamamoto, S.; Ejaz, M.; Tsujii, Y.; Fukuda, T. *Macromolecules* **2000**, *33*, 5608 (part 2 of this series of papers).
(38) Cleaveland, J. P.; Manne, S.; Bocek, D.; Hansma, P. K. *Rev. Sci. Instrum.* **1993**, *64*, 403.
(39) Ducker, W. A.; Sendan, T. J.; Pashley, R. M. *Langmuir* **1992**, *8*, 1831.
(40) We measured force curves after the cantilever was immersed for a certain period of time in the solvent. The obtained force curves were exactly the same independent of the immersion time. This shows that Araldite is inert under the present experimental condition.
(41) Hues, S. M.; Draper, C. F.; Lee, K. P.; Colton, R. J. *Rev. Sci. Instrum.* **1994**, *65*, 1561.
(42) Comstock, R. H. US Patent 4263527, 1981.
(43) Jaschke, M.; Butt, H.-J. *Rev. Sci. Instrum.* **1995**, *66*, 1258.
(44) Butt, H.-J.; Kappl, M.; Mueller, H.; Raiteri, R.; Meyer, W.; Rühe, J. *Langmuir* **1999**, *15*, 2559.
(45) The measurement time scale (scan speed) employed in imaging was comparable to that employed in the force measurements. A scan speed 10 times faster than this gave the same D_o within an experimental error.
(46) Alexander, S. *J. Phys. (Paris)* **1977**, *38*, 983.
(47) (a) Milner, S. T.; Witten, T.; Cates, M. *Macromolecules* **1988**, *21*, 2610. (b) Milner, S. T. *Europhys. Lett.* **1988**, *7*, 695. (c) Milner, S. T.; Witten, T. A.; Cates, M. E. *Macromolecules* **1989**, *22*, 853.
(48) This value was obtained from the data reported by Hadziioannou et al.[12] and Taunton et al.[14]
(49) de Gennes, P. G. *Adv. Colloid Interface Sci.* **1987**, *27*, 189.

MA991733A